Arab J Geosci (2015) 8:6095–6104
DOI 10.1007/s12517-014-1614-5

ORIGINAL PAPER

Origin of the mafic dykes in Nagarparker area of Pakistan

Tahseenullah Khan · Mamoru Murata · Muhammad Zafar · Hafiz Ur Rehman

Received: 13 May 2014 / Accepted: 1 September 2014 / Published online: 10 September 2014

Abstract The Nagarparker area of Pakistan comprises igneous and metamorphic rocks dissected by coarse-grained gabbro dykes and medium- to fine-grained dolerites at Karai, Dhedvero, and the central part of the area. The gabbro dykes contain plagioclase (An_{79}), diopside, diopsidic-augite, and olivine with minor biotite, magnetite, ilmenite, titanite, and ilmenite-titanite composite grains. The dolerites consist of plagioclase, titaniferous augite, augite, hornblende, biotite, titanite, apatite, zircon, titanomagnetite, rutile, and ilmenite. Based on geochemistry, the gabbro dykes (group I) and dolerites (group II) are classified as subalkaline whereas group III dolerites as alkaline. In spidergram, Nb troughs and Sr crests are depicted in the group I and group II dykes whereas the group III dykes illustrate positive Nb and negative Sr with relatively smooth trace element pattern. The mineralogical composition, discriminant quadratic analysis, and trace element variations distinguish the mafic dykes of the study area into two magmatic groups. The first group comprises group I and group II dykes which depict island-arc type whereas the group III dykes resemble OIB-type compositions similar to Seychelles islands and the Tavidar region of Indian Rajasthan. The tentative timing of their emplacement may be Neoproterozoic and Cretaceous (?), respectively.

T. Khan (✉) · M. Zafar
Department of Earth and Environmental Sciences, Bahria University, Shangrilla Road, Sector E-8, Islamabad, Pakistan
e-mail: dr.tahseen@bui.edu.pk

M. Murata
Department of Geosciences, Faculty of Science, Naruto University of Education, National University Corporation, Naruto, Tokushima 772-8502, Japan

H. U. Rehman
Department of Earth and Environmental Science, Faculty of Science, Kagoshima University, Kagoshima 890-0065, Japan

Keywords Nagarparker · Mafic dykes · Origin · Tectonic setting · Pakistan

Introduction

Mafic dykes are common appearance of crustal extension and short-lived magmatic events of the migration of basaltic magma from mantle to upper crust carrying important temporal and chemical constraints for the evolution of the lithospheric mantle (Wilson 1989; Maurice et al. 2009). In the Nagarparker area, mafic dykes extensively dissect the Precambrian igneous and metamorphic rock assemblages of the Indian shield. This rock assemblage was named as the Nagar Parkar igneous complex by Kazmi and Khan (1973). Based on similarity in rock assemblages, the Nagarparker area was correlated with the adjacent northwest Indian Rajasthan, the Seychelles islands, and Madagascar (e.g., Ashwal et al. 2002; Khan et al. 2012). The present study incorporates detailed field, petrological, and geochemical (in particular trace element) data of the mafic dykes from the entire Nagarparker area. For comparison, geochemical data of the mafic rocks of the Seychelles islands, Kohistan island arc, and Ladakh Himalaya, LEG 176 and the Tavidar region of the Indian Rajasthan are incorporated to ascertain the petro-tectonic evolution of the mafic dykes of the Nagarparker area.

Outline of geology

The Nagarparker area lies in the extreme southeast corner of Pakistan bordering India (Fig. 1), which is believed to be the western continuation of the Precambrian Indian shield (Pathan and Rais 1975; Ahmad and Chaudhry 2007, 2008; Khan et al. 2012). Kazmi and Khan (1973) presented a geological map of the area and reported the Quaternary deposits, subordinate

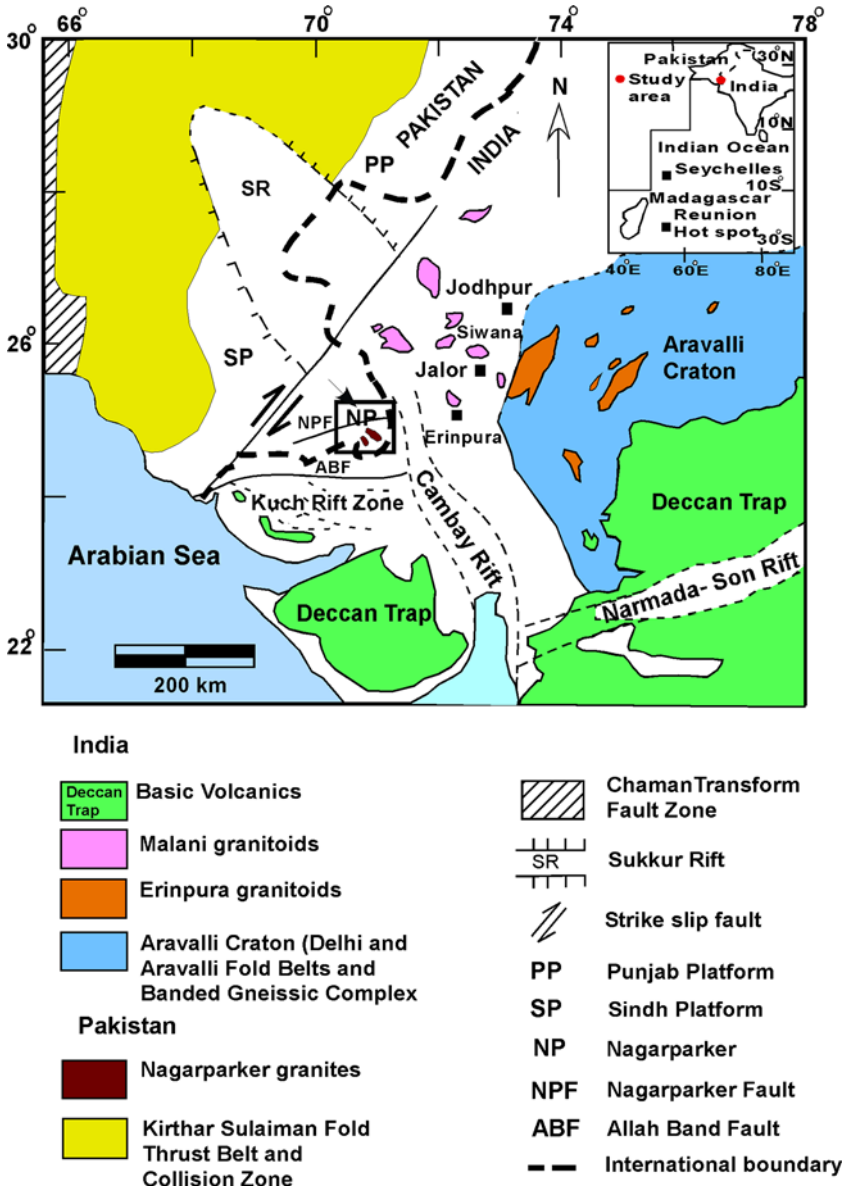

Fig. 1 A simplified regional map showing the tectonic configuration and geographical position of Nagarparker in the Indian shield (after Raza et al. 1989; Biswas 2005; Khan et al. 2012). *Small square box* in the middle shows the Nagarparker area. *Inlet* in the *upper right* shows the geographical location of the study area and those of Seychelles and Madagascar

Jurassic-Tertiary sandstone, and clay, overlying basement and divided the area into Dhedvero basic intrusions, Nagarparker pink granite, and Karunjhar gray granite (Fig. 2).

To the southeast of the Dhedvero and west of Berana, particularly in the vicinity of Walo jo Wandio (Fig. 2) and Moti jo Wandio (not shown in the map), there exist small exposures of schists, paragneisses, migmatites, and quartzites, which were not reported earlier. Such an exposure of a 75-m long and 10-m wide quartzite body has been noticed as xenoblock within coarse-grained pink granite at Moti jo Wandio (24° 24′ 28″ latitude and 70° 57′ 14″ longitude). The paragneisses strike N50° W with 55° SW dip. These metasedimentary rock assemblages along with amphibolites are intruded by pink granites and mafic and acidic dykes. The metamorphic rocks, the intruded granites, and mafic dykes are partially sheared and deformed. Khan et al. (2012) divided the Nagarparker granites into five rock units, namely pink, reddish pink, pinkish gray, gray, and grayish white granites based on field observations and mineral and geochemical compositions. There are slight variations in mineralogy and geochemistry among the pink granites; however, these differ from gray and grayish white granites. The pink granites contain braided, albitized perthites and perthitized microcline, intergranular and graphic quartz, biotite, magnetite, titanite, apatite, zircon, and monazite±fluorite±hornblende±riebeckite and impart rapakivi and myrmekitic textures. Gray granites contain braided perthite, perthitic albite, quartz, ferro-richterite, riebeckite± arfvedsonite, rutile, and allanite besides common accessory minerals in both types. The grayish white granites contain K-feldspar as microcline, quartz, and discrete albite twinned

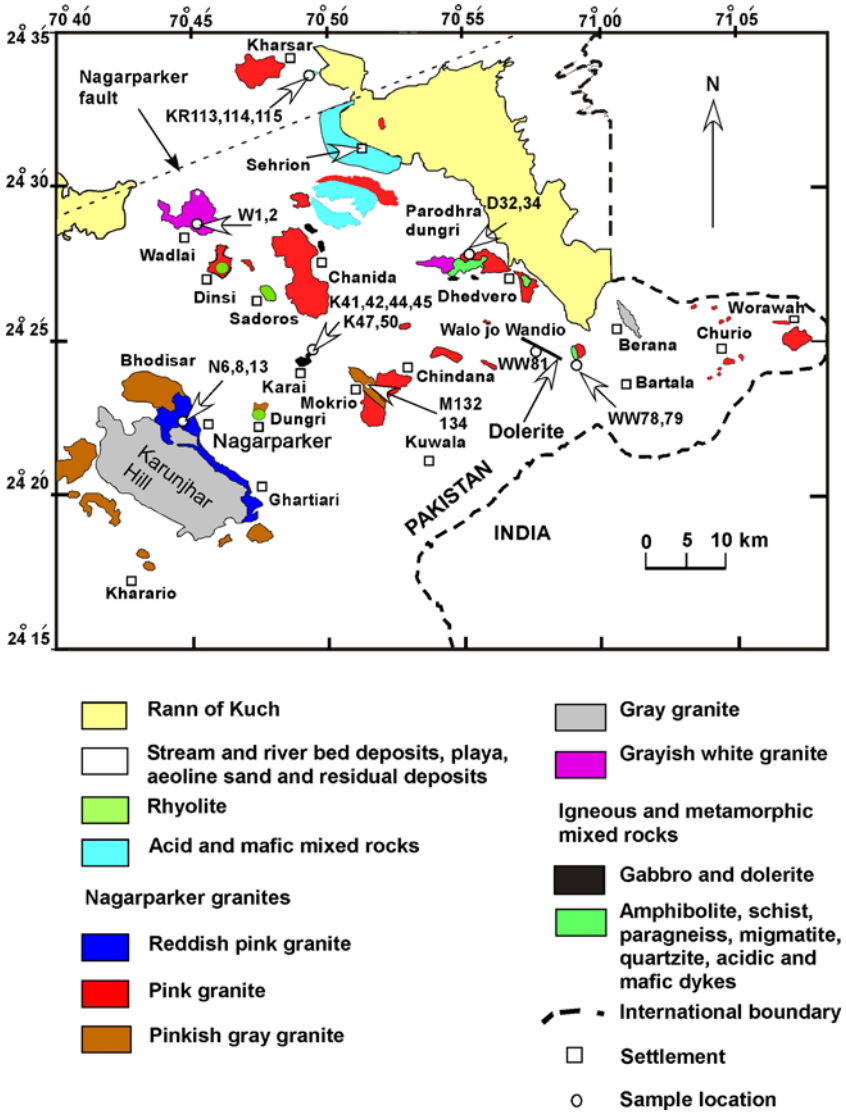

Fig. 2 Geological map of Nagarparker, Sindh province of Pakistan (after Jan et al. 1997; Muslim et al. 1997; Muhammad and Alizai 2007; Ahsan et al. 2008; Khan et al. 2012)

plagioclase grains with common biotite and minor hornblende. The pink granites and gray granites yield ~750 and 1100 Ma radiometric ages, respectively (e.g., Khan et al. 2012).

Field features and petrography of the mafic dykes

Mafic dykes occur at Karai, Dhedvero, and the central part of the Nagarparker area (e.g., Jan et al. 1997; Ahmad and Chaudhry 2007; Laghari et al. 2013 (Fig. 2). These are medium- to fine-grained dolerites and a few coarse-grained gabbro dykes. The gabbro dykes at Karai intrude the dolerites. These gabbro dykes contain plagioclase (An_{79}), diopside, diopsidic-augite, and olivine. Biotite occurs in subordinated amounts and surrounds the olivine and clinopyroxene grains (Fig. 3a). In sample K44, clinopyroxene occurs as oikocryst containing plagioclase (Fig. 3b). Magnetite, ilmenite, titanite, and ilmenite-titanite composite grains occur as accessory oxide phases in these dykes. Medium- to fine-grained dolerites occur in a wide area. At Karai, the dolerites are about 20 m wide and 50 m long trending in N40° W and N30° E directions intruding amphibolites and gabbros (Fig. 4a–b). These dolerites contain plagioclase, titaniferous augite, hornblende, biotite, and titanite. Apatite and zircon occur as accessories. Magnetite, hematite, titanomagnetite, ilmenite, pyrite, and chalcopyrite are the opaques. Medium- to fine- grained dolerites also intrude 1100- to ~750-Ma old gray, pink, and grayish-white granites (Figs. 4c–d) and pink granite at Nagarparker, Mokrio, Kharsar, Wadali, amphibolites, and metasedimentary rocks at Dhedvero, Walo jo Wandio, and the surroundings. These dolerites trend in NW–SE direction with nearly vertical dips and are about 1 to 3 m wide and 5 to 10 m long. At Wadlai, a 75-m long and 4-m wide dolerite dissects the grayish white granite whereas at Walo jo Wandio, a 3-km long and 40- to 60-m wide dolerite trails nearly in east–west direction.

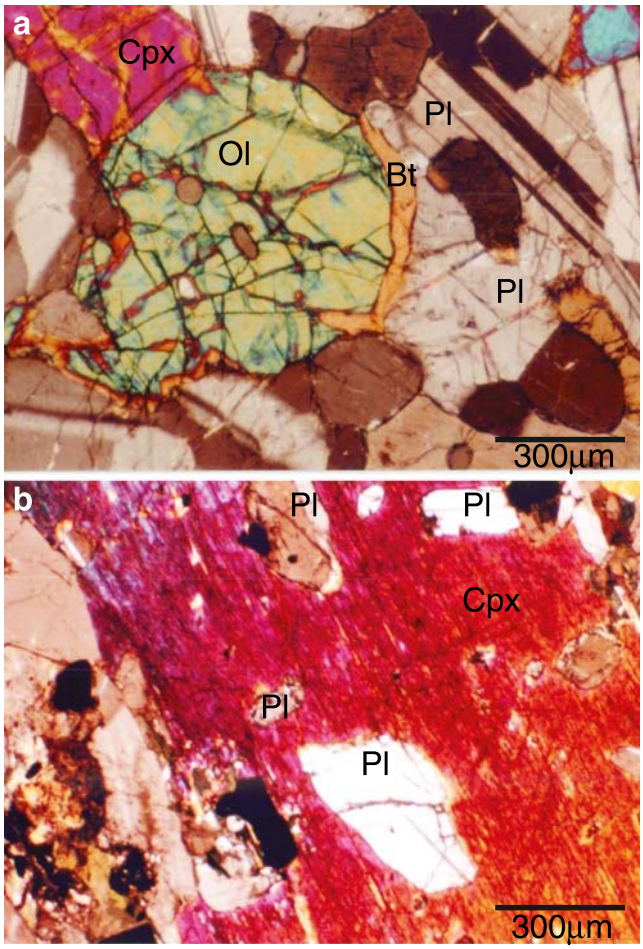

Fig. 3 **a** Photomicrograph of gabbro dyke (sample K47) illustrating olivine, clinopyroxene, and plagioclase. Olivine contains plagioclase as inclusions. Biotite is developed rimming the olivine and clinopyroxene grains. All photomicrographs are taken in crossed polars. **b** Photomicrograph of gabbro dyke (sample K44) showing clinopyroxene oikocryst containing plagioclase

In thin sections, these dolerites are subophitic to ophitic and contain plagioclase, hornblende, and augite as main minerals. Plagioclase is partly altered to sericite, calcite, and epidote and hornblende to biotite and chlorite. Magnetite, titanomagnetite, and pyrite occur as minor opaques and zircon and apatite as accessories. Some of these dolerites intruding the deformed pink granites are also deformed (Fig. 5a). In one of the dyke sample N8, quartz grains occur as interstitial mass and megacrysts. The quartz megacryst in sample N8 is fractured due to stresses (Fig. 5b). This dyke intrudes reddish pink granite of 750-Ma age at the Nagarparker.

Analytical methods

Twenty-one rock samples including four gabbro dykes and seventeen dolerites were analyzed for major element oxides and trace element compositions by using Rigaku System 3370 X-ray fluorescence spectrometer (XRF) in the Geoscience Laboratory, Geological Survey of Pakistan, Islamabad (Table 1). Powdered rock samples mixed with 10 times weight of lithium tetraborate were fused to make a glass disk for major element analysis. Thirty-two USGS and GSJ standard reference samples were used for the calibration of the instrument. For trace and rare-earth element analysis, powdered samples were compressed. The same standard samples, used for major elements, were also used for the empirical method with matrix and overlapping corrections (Murata 1993). Mineral chemistry data of olivine, clinopyroxene, plagioclase, and opaque oxides were also produced in these mafic dykes by using electron probe micro-analyzer (EPMA) JEOL Superprobe System at the Department of Geosciences, Naruto University of Education, Tokushima, Japan, which are incorporated in the text (Table 2).

Geochemical results

Whole rock geochemistry

As most of the mafic dykes are partially altered, therefore, high-field-strength elements (HFSE) are used for their geochemical classification. On the basis of the Nb/Y and Zr/TiO_2 plot, the mafic dykes both gabbros and dolerites plot in two domains, i.e., subalkaline and alkaline. Gabbro dyke samples K44, K47, K50, and W1 and dolerites samples N6, N8, N13, N45, KR114, M132, M134, W2, WW78, and WW79 plot as subalkaline whereas dolerites samples K41, KR113, KR115, WW81, D32, and D34 plot as alkaline except sample K42 which plots in subalkaline field due to relatively high values in TiO_2 (4 wt%) and Y (32 ppm) (Fig. 6a). On the basis of alkaline and subalkaline nature of the studied dykes, these are differentiated as group I (subalkaline) gabbro dykes and group II (subalkaline) and group III (alkaline) dolerites. To know the magmatic parentage of dolerite sample K42, Maruyama (1976) diagram has been employed (Fig. 6b). Three of the analyzed spots of the cores of Ti-augite show higher total Al and Ti contents in sample K42 reflecting its alkaline nature. The other two analyzed spots of the margins of the Ti-augite in sample K42 show lower values in total Al and Ti due to fractionation and plot with gabbro dykes (Fig. 6b). In SiO_2 versus MgO diagram, the group I gabbro dykes and group II dolerites (subalkaline) overlap whereas the group III dolerites (alkaline) plot in a separate domain except sample K41, which plots away due to relatively higher MgO content (9.21 wt%; Fig. 7).

Spider diagram

Trace element abundances are well illustrated in the mafic dykes when normalized to N-MORB values of Sun and

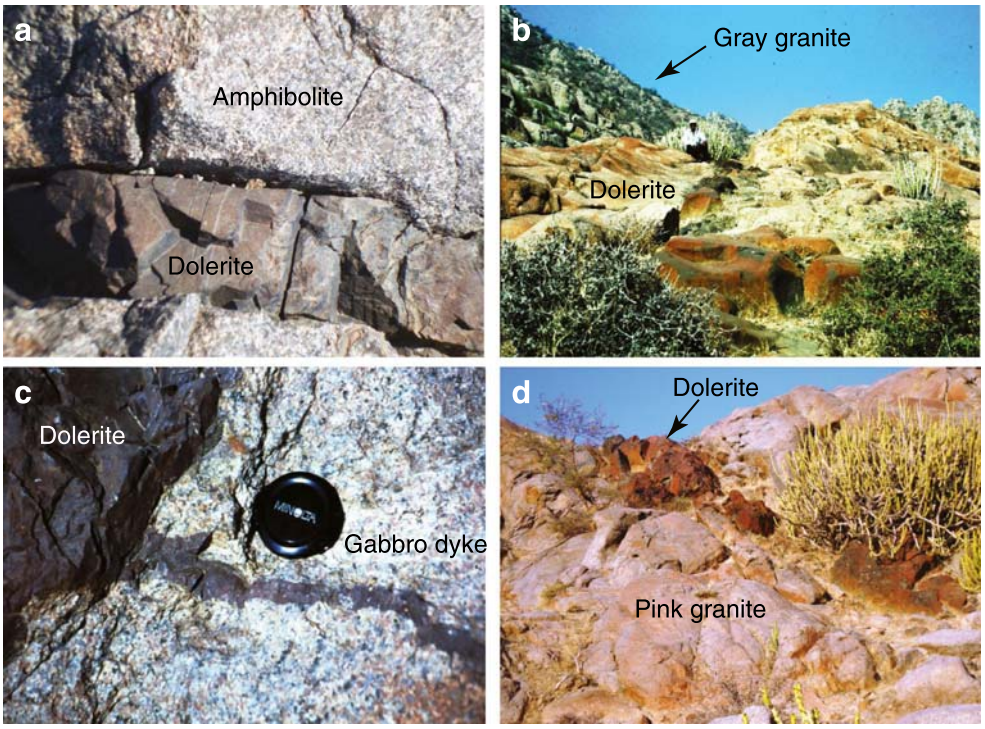

Fig. 4 Dolerite intruding amphibolites at Dhedvero (**a**). Dolerite intruding gabbro dyke at Karai (**b**) (Khan et al. 2012). Dolerite intruding gray granite at Nagarparker (**c**). Dolerite intruding pink granite at Mokrio (**d**)

McDonough (1989) (Fig. 8a–c). The group I dykes show enrichment in Ba, K, Rb, and Th as compared to Nb, Sr, Ce, P, Ti, and Y with marked negative anomaly at Nb (Fig. 8a). The group II dykes are more enriched in trace elements as compared to group I, illustrating a similar geochemical trend (Fig. 8b). The group III dykes depict more enrichment in trace elements as compared to the group I and group II dykes with nearly smooth geochemical pattern (Fig. 8c). On these spidergrams (Fig. 8a–c), the group I and group II dykes exhibit island-arc type whereas the group III dykes illustrate OIB-type geochemical signatures (e.g., Pearce 1982; Wilson 1989).

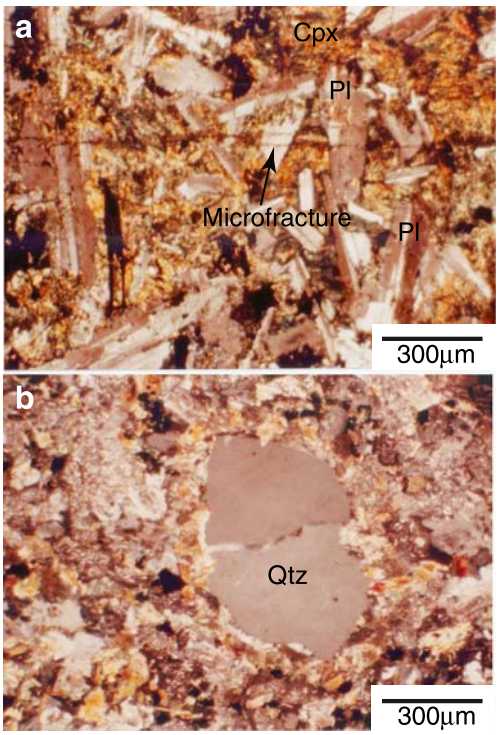

Fig. 5 **a** Photomicrograph of dolerite (sample WW79) showing deformation as depicted by microfracture in the rock. The bulk of the rock comprises plagioclase, clinopyroxene, hornblende, biotite, and opaques. **b** Photomicrograph of dolerite (sample N8) depicting deformed quartz phenocryst in altered ground mass

Magma source

The group I and group II dykes occupy island arc field except samples N6, N8, N13, and N45 of group II dykes which seem to be geochemically more evolved and/or altered rocks, plot in MORB and OIB fields, on quadratic discriminant analysis diagram using Na, Nb, and Sr as discriminants (e.g., Vermeesch 2006; Fig. 9a). The group III dykes are generally restricted to OIB field. The group I dykes exhibit higher Sr/Y ratio and low Y contents that resemble adakitic-type rocks (e.g., Castillo 2006); however, the higher abundance of Sr may be attributed to the late fractionation of plagioclase under high water pressure (e.g., Yoder and Tilley 1962). On the Zr-Nb-Y ternary diagram of Meschede (1986), the group III dykes distinctly plot within plate fields and the group I and group II dykes in volcanic arc basalt fields (Fig. 9b).

Table 1 Major oxides (wt %) and trace elements (ppm) whole rock chemistry of the gabbro dykes and dolerites

	Subalkaline gabbro dykes (group I)				Subalkaline dolerites (group II)										Alkaline dolerites (group III)						
Sample	K44	K47	K50	W1	N6	N8	N13	K45	W2	KR114	M132	M134	WW78	WW79	K41	K42	KR113	KR115	WW81	D32	D34
SiO_2	48.18	43.74	48.34	51.22	54.32	56.71	49.87	53.78	49.48	48.92	48.31	52.34	50.03	48.00	45.70	44.90	46.91	47.71	46.22	47.57	47.22
TiO_2	1.57	0.20	1.76	1.58	2.04	1.86	2.35	2.24	2.33	2.20	2.53	1.57	1.41	3.36	2.23	4.00	3.00	2.81	2.80	3.41	3.51
Al_2O_3	17.48	17.68	16.58	16.38	14.71	14.71	15.54	15.26	15.86	15.62	15.33	15.99	17.71	15.58	15.31	15.21	16.32	16.06	14.35	16.22	16.74
Fe_2O_3	11.06	12.97	10.33	10.91	12.34	11.22	13.84	11.26	12.04	12.49	13.21	10.16	9.58	12.24	12.14	17.76	15.92	14.34	14.94	15.58	14.39
MnO	0.13	0.16	0.15	0.18	0.17	0.17	0.21	0.16	0.17	0.17	0.20	0.17	0.12	0.12	0.18	0.24	0.17	0.18	0.20	0.31	0.17
MgO	6.79	13.57	6.37	6.55	4.52	4.04	5.72	5.09	5.83	7.06	6.37	5.13	7.11	6.72	9.21	5.82	3.79	3.38	5.61	4.89	5.10
CaO	12.56	10.99	13.74	8.68	6.35	5.54	7.35	7.18	7.45	8.70	8.39	7.82	10.10	9.38	12.48	7.97	5.62	6.62	10.94	7.12	7.99
Na_2O	1.92	0.65	2.25	3.60	3.04	3.18	2.95	3.63	4.38	3.14	3.42	4.60	3.16	3.23	2.21	2.87	4.43	5.63	3.01	3.32	3.06
K_2O	0.27	0.01	0.38	0.60	2.13	2.21	1.69	0.85	1.87	1.19	1.67	1.78	0.57	0.56	0.26	0.46	2.78	1.84	1.13	1.06	1.38
P_2O_5	0.04	0.03	0.10	0.30	0.38	0.36	0.48	0.55	0.59	0.50	0.57	0.44	0.21	0.81	0.28	0.77	1.06	1.43	0.80	0.52	0.44
Total	100	100	100	100	100	100	100	100	100	100	100	100	100	100	100	100	100	100	100	100	100
LOI	1.57	1.46	1.08	1.45	1.76	1.67	1.36	1.59	1.18	1.77	1.82	0.80	1.08	1.56	5.52	2.84	2.65	3.02	0.04	6.28	6.75
Nb	1	traces	2	2	11	12	15	7	5	4	5	6	2	6	13	13	33	29	23	24	24
Zr	33	22	45	98	263	255	251	266	206	189	237	152	98	242	167	315	334	399	105	220	213
Y	12	8	14	18	38	41	38	29	24	24	26	25	19	28	18	32	22	22	21	21	19
Sr	409	446	408	382	259	253	336	348	639	420	408	278	418	387	322	400	744	688	458	342	754
Rb	7	4	10	12	49	61	69	12	46	31	47	118	14	18	6	6	40	22	23	25	22
Ba	93	17	96	196	329	328	380	406	692	712	404	150	204	278	104	247	569	547	863	190	254
V	311	149	312	[a]	244	289	294	259	[a]	[a]	[a]	[a]	[a]	[a]	274	272	[a]	[a]	[a]	231	231
Co	67	89	46	[a]	43	49	44	62	[a]	[a]	[a]	[a]	[a]	[a]	48	38	[a]	[a]	[a]	42	50
Cr	267	58	[a]	122	71	58	97	82	174	217	162	169	194	162	383	26	1	230	62	109	70
Ni	32	247	77	58	49	42	63	62	46	126	72	51	82	81	176	30	2	traces	39	72	61
Ga	[a]	13	17	[a]	21	23	23	20	[a]	[a]	[a]	[a]	[a]	[a]	19	24	20	20	20	19	17
Ce	[a]	[a]	[a]	[a]	61	49	37	73	42	36	40	32	[a]	40	43	60	81	97	57	77	43
Nd	[a]	[a]	[a]	[a]	49	34	37	[a]	[a]	[a]	[a]	[a]	[a]	[a]	[a]	39	[a]	[a]	[a]	34	35
Sr/Y	34	56	29	21	7	6	9	12	27	18	16	11	23	14	18	13	34	31	21	16	40

Fe_2O_3 expressed as total iron; major elements oxides normalized to total 100 %

Detection limits are as follows: 1 ppm for Nb, Zr, Y, Sr, Rb, Ni, Cr, and Co; 24 ppm for Ba; 7 ppm for V; 30 ppm for Ce and Nd. Samples analyzed on dry basis and loss on ignition (LOI) determined at 1000 °C

K Karai, *N* Nagarparker, *W* Wadlai, *KR* Kharsar, *M* Mokrio, *WW* Walo jo Wandio, *D* Dhedvero

[a] Under detection limit

Table 2 The representative microprobe analyses of clinopyroxene of the gabbro dykes and dolerites

Subalkaline gabbro dykes (group I)																	
Sample	K44c	K44m	K44c	K44m	K44m	K44m	K47c	K47m	K50c	K50m	K50m	K50c	K50m	K47c	K47m	K47c	K47m
SiO_2	50.89	50.35	51.12	50.70	50.97	50.20	51.13	51.27	52.33	51.62	52.32	51.96	51.83	50.44	48.51	50.03	50.46
TiO_2	1.26	1.28	0.99	1.25	1.29	1.11	1.15	1.14	0.62	0.82	0.57	0.51	0.57	1.03	1.36	1.36	1.09
Al_2O_3	3.07	3.17	2.75	3.00	3.18	2.89	3.42	3.34	2.00	2.36	1.61	1.95	2.01	2.75	3.75	3.56	3.14
FeO	7.85	7.58	7.06	7.13	7.07	6.60	8.05	7.61	7.33	7.80	7.44	8.02	7.67	7.55	9.22	7.74	7.19
Cr_2O_3	tr	0.02	0.05	tr	0.05	0.04	0.06	tr	0.07	tr	0.03	tr	0.03	tr	0.03	tr	0.03
MnO	0.28	0.15	0.30	0.26	0.23	0.13	0.22	0.16	0.24	0.31	0.24	0.27	0.23	0.16	0.22	0.19	0.19
MgO	15.10	14.33	15.49	14.62	15.28	14.92	15.58	14.99	15.65	15.07	15.01	15.37	15.44	14.63	14.83	14.39	15.09
CaO	21.73	22.46	22.18	22.82	22.04	23.18	21.28	21.70	21.53	22.45	22.60	22.48	22.65	22.77	20.45	22.32	22.08
Na_2O	0.40	0.39	0.44	0.47	0.47	0.44	0.32	0.31	0.41	0.41	0.34	0.36	0.33	0.39	0.35	0.46	0.37
K_2O	tr	0.03	tr	tr	tr	tr	tr	0.02	0.01	tr	tr	tr	tr	tr	tr	tr	tr
TSi	1.870	1.869	1.876	1.869	1.868	1.859	1.865	1.885	1.925	1.892	1.932	1.902	1.899	1.870	1.821	1.850	1.867
TAl	0.130	0.131	0.119	0.130	0.132	0.126	0.135	0.115	0.075	0.102	0.068	0.084	0.086	0.120	0.166	0.150	0.133
TFe3	tr	tr	0.005	0.001	tr	0.015	tr	tr	tr	0.006	tr	0.014	0.015	0.010	0.013	tr	tr
M1Al	0.003	0.008	tr	tr	0.005	tr	0.011	0.030	0.011	tr	0.002	tr	tr	tr	tr	0.005	0.004
M1Ti	0.035	0.036	0.027	0.035	0.036	0.031	0.032	0.032	0.017	0.023	0.016	0.014	0.016	0.029	0.038	0.038	0.030
M1Fe3	0.085	0.080	0.099	0.095	0.087	0.109	0.081	0.045	0.057	0.091	0.058	0.095	0.092	0.099	0.127	0.102	0.094
M1Fe2	0.049	0.083	0.025	0.067	0.036	0.035	0.025	0.073	0.055	0.061	0.097	0.052	0.047	0.063	0.004	0.060	0.037
M1Cr	tr	0.001	0.002	tr	0.001	0.001	0.002	tr	0.002	tr	0.001	tr	0.001	tr	0.001	tr	0.001
M1Mg	0.827	0.793	0.847	0.803	0.835	0.824	0.847	0.821	0.858	0.823	0.826	0.838	0.843	0.809	0.830	0.793	0.832
M2Fe2	0.107	0.073	0.088	0.057	0.094	0.045	0.139	0.117	0.114	0.080	0.074	0.085	0.080	0.062	0.145	0.077	0.092
M2Mn	0.009	0.005	0.009	0.008	0.007	0.004	0.007	0.005	0.007	0.009	0.007	0.008	0.007	0.005	0.007	0.006	0.006
M2Ca	0.856	0.893	0.872	0.901	0.866	0.920	0.832	0.855	0.849	0.882	0.894	0.882	0.889	0.905	0.822	0.884	0.875
M2Na	0.029	0.028	0.031	0.034	0.033	0.031	0.023	0.022	0.030	0.029	0.024	0.025	0.024	0.028	0.026	0.033	0.027
M2K	tr	0.001	tr	tr	tr	tr	tr	0.001	tr	tr	tr	tr	tr	tr	tr	tr	tr

Subalkaline gabbro dykes (group I)					Subalkaline dolerites (group II)					Alkaline dolerites (group III)					
Sample	K44c	K44m1	K44m2	K44c	K44m	N8c	N8c	N8m	N8m	N8c	K42m	K42c	K42c	K42c	K42m	K42m
SiO_2	51.16	50.88	50.78	50.97	51.20	49.71	50.54	51.53	51.20	51.03	50.02	49.02	49.03	50.95	49.86	50.11
TiO_2	1.07	1.10	1.31	1.23	1.08	1.33	0.98	1.01	1.14	1.07	1.64	2.06	1.78	1.11	1.06	0.96
Al_2O_3	2.96	2.95	3.30	3.10	2.61	3.23	2.48	2.64	2.79	2.84	3.54	4.58	4.28	2.33	3.00	2.17
FeO	7.65	7.26	6.93	7.15	8.01	11.27	10.63	10.02	11.24	10.23	11.72	11.38	10.96	11.03	13.47	10.81
Cr_2O_3	0.01	0.04	0.03	0.04	0.05	0.08	0.08	0.03	tr	0.06	tr	tr	tr	tr	tr	0.21
MnO	0.24	0.19	0.14	0.20	0.25	0.25	0.22	0.23	0.36	0.29	0.29	0.17	0.27	0.29	0.31	0.30
MgO	15.17	14.86	15.30	15.14	15.75	15.33	15.80	15.53	15.59	15.43	12.30	12.57	13.30	13.90	12.17	13.45
CaO	21.07	22.03	20.96	22.29	21.41	18.91	17.32	19.48	18.74	19.42	21.17	20.49	20.64	20.33	18.80	19.93
Na_2O	0.47	0.37	0.38	0.50	0.39	0.40	0.34	0.36	0.32	0.33	0.72	0.49	0.58	0.51	0.56	0.46
K_2O	tr	0.01	0.02	0.01	0.02	tr	tr	0.02	tr	tr	tr	tr	tr	tr	0.07	tr
TSi	1.892	1.886	1.887	1.867	1.874	1.839	1.906	1.895	1.879	1.882	1.855	1.828	1.817	1.896	1.896	1.906
TAl	0.108	0.114	0.113	0.133	0.112	0.141	0.094	0.105	0.121	0.118	0.145	0.172	0.183	0.102	0.104	0.094
TFe3	tr	tr	tr	tr	0.013	0.020	tr	tr	tr	tr	tr	tr	tr	0.002	tr	tr
M1Al	0.021	0.014	0.032	0.001	tr	tr	0.016	0.010	tr	0.005	0.009	0.029	0.004	tr	0.030	0.003
M1Ti	0.030	0.031	0.037	0.034	0.030	0.037	0.028	0.028	0.031	0.030	0.046	0.058	0.049	0.031	0.030	0.028
M1Fe3	0.061	0.064	0.035	0.099	0.092	0.113	0.045	0.064	0.081	0.075	0.096	0.062	0.121	0.078	0.057	0.063
M1Fe2	0.052	0.069	0.048	0.037	0.015	0.002	0.021	0.045	0.035	0.040	0.169	0.152	0.089	0.120	0.192	0.137
M1Cr	tr	0.001	0.001	0.001	0.002	0.002	0.002	0.001	tr	0.002	tr	tr	tr	tr	tr	0.006
M1Mg	0.836	0.821	0.848	0.827	0.860	0.845	0.888	0.852	0.853	0.848	0.680	0.699	0.735	0.771	0.690	0.763
M2Fe2	0.124	0.092	0.132	0.083	0.124	0.214	0.269	0.198	0.229	0.200	0.099	0.141	0.130	0.144	0.179	0.144
M2Mn	0.007	0.006	0.004	0.006	0.008	0.008	0.007	0.007	0.011	0.009	0.009	0.005	0.008	0.009	0.010	0.010
M2Ca	0.835	0.875	0.835	0.875	0.840	0.750	0.700	0.768	0.737	0.767	0.841	0.819	0.820	0.811	0.766	0.812
M2Na	0.034	0.026	0.028	0.035	0.027	0.028	0.024	0.026	0.023	0.024	0.052	0.035	0.042	0.037	0.042	0.034
M2K	tr	tr	0.001	tr	0.001	tr	tr	0.001	tr	tr	tr	tr	tr	tr	0.003	tr

Location “c” stands for “core” and “m” for “margin” of the EPMA spot analyses on clinopyroxene grains. “tr” stands for “traces.” “T” refers to cations coordinated in tetragonal “T” site, “M1” refers to “Y” site where cations are coordinated in octahedral site, and “M2” refers to “X” site where cations can be coordinated with six or eight oxygen atoms depending upon the cation size

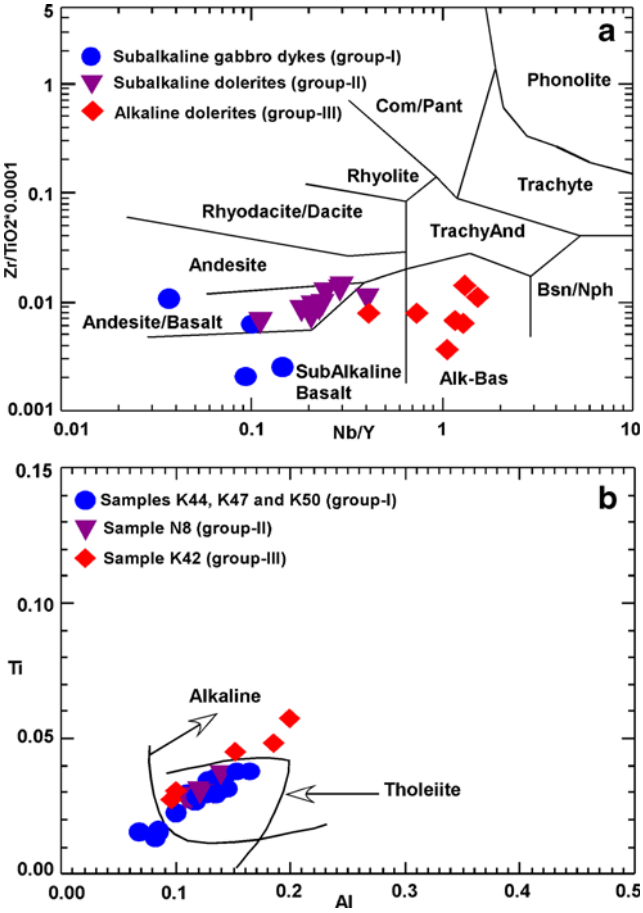

Fig. 6 **a** Rock classification of Winchester and Floyd (1977) showing the composition of gabbro dykes and dolerites as subalkaline (group I and group II) and alkaline (group III), respectively, from the Nagarparker area. **b** Al_{total} versus Ti diagram using clinopyroxene composition to discriminate between gabbro dykes and dolerite (K42) into subalkali and alkali types

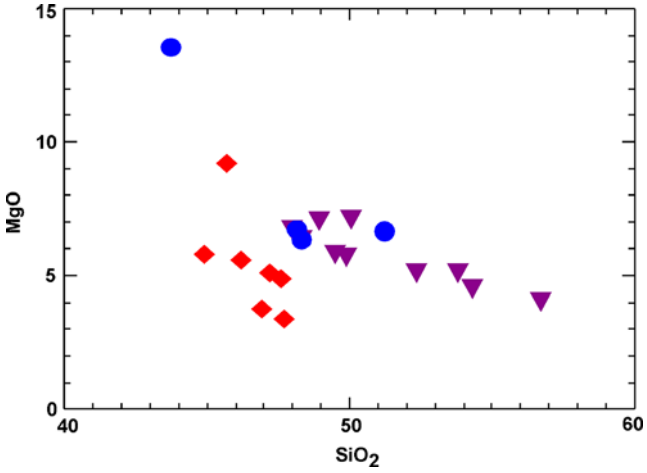

Fig. 7 SiO_2 versus MgO diagram showing the composition of subalkaline gabbro dykes and dolerites (group I and group II) and alkaline dolerites (group III) of the Nagarparker area

Discussion

The Nagarparker area consists of granites of island arc crust composition equivalent to granites of the Seychelles islands which, according to Khan et al. (2012), represent the Rodinia remnants. The basements are intruded by gabbro dykes and dolerites, i.e., group I, group II, and group III dykes. Their tectonic settings have been evaluated by comparing these rocks with the tectonically well-known regions. For example, the mafic dykes of the Kohistan island arc intruding the subduction-related Kohistan batholith and the mafic-ultramafic rocks of the Chilas complex are typical of island arc composition (e.g., Khan et al. 1993; Mikoshiba et al. 1999; Takahashi et al. 2007; Khan et al. 2011). The OIB-type gabbros of Ladakh Himalaya of Sinha and Mishra (1994) and the Tavidar mafic volcanic suite of Sen et al. (2012) resemble the group III dykes of the Nagarparker area. The LEG 176 gabbros of Niu et al. (2002) represent typical MORB composition, which differ from the Nagarparker mafic dykes.

Similar aphyric mafic dykes trending east–west are also reported from the Seychelles islands (e.g., Ashwal et al. 2002). For example, two dolerite dykes up to 40 cm thick intruding tuffs have been reported at Pointe Vareur and pointe Zeng Zeng in the Silhouette Island of the Seychelles, which are dissected by microsyenite (Owen-Smith et al. 2013). The dolerites in the Seychelles island yield late Precambrian age of ~750 Ma and a few late Cretaceous (Torsvik et al. 2001; Ashwal et al. 2002). The Silhouette and North islands of Seychelles represent 63- to 63.5-Ma-old alkaline plutonic volcanic complexes, similar to the Deccan trap-like magmatism of the Reunion hotspot (Owen-Smith et al. 2013). Such Proterozoic and Cretaceous subduction and plume-related mafic dykes, respectively, are also reported from the southern margin of Cuddapah Basin, India, by Goutham et al. (2010).

The mafic dykes of the Nagarparker area have not been dated yet, but due to lithological and geochemical resemblances, the group II dykes of the study area may be correlated tentatively with the subalkaline dolerites of Seychelles islands. The Seychelles islands according to Ashwal et al. (2002) represent an Andean-type continental arc.

Other supporting evidence is the presence of mixed rocks of metaigneous (amphibolites), metasedimentary (schist, paragneiss, migmatite, and quartzite), and calc-alkaline to tholeiitic magmatic rocks in the Dhedvero and the surrounding areas of Nagarparker. Similar rock assemblages are also reported from the Sahantaha Group of continental crust and the juvenile Neoproterozoic Bemarivo Belt arc system of northern Madagascar (e.g., Jöns et al. 2006; Thomas et al. 2009; Fritza et al. 2013). On the basis of common occurrence of ~750-Ma magmatic rocks, the Bemarivo Belt has been

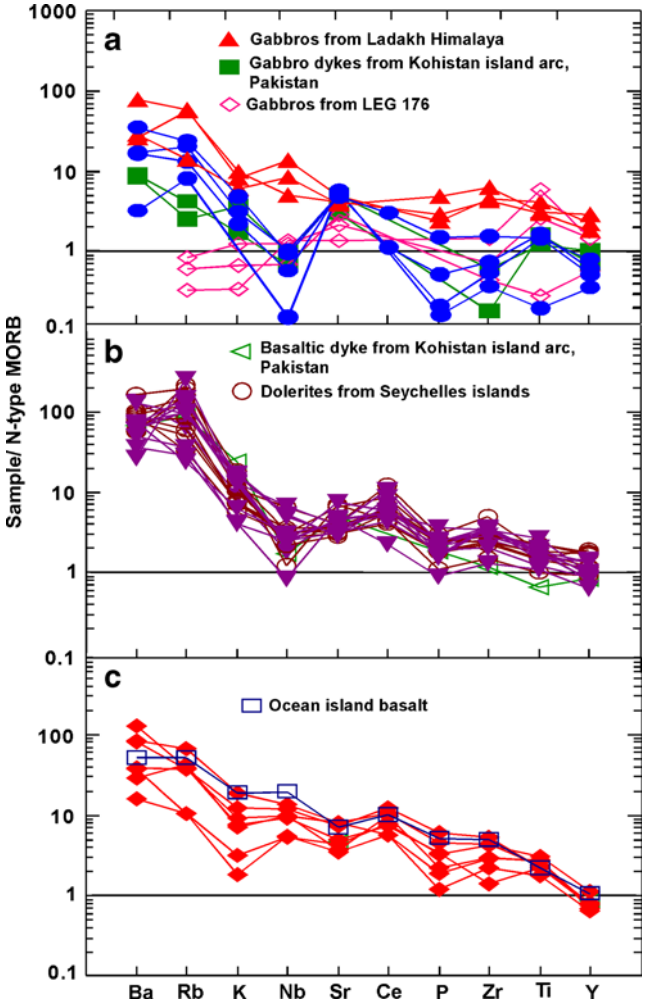

Fig. 8 N-MORB normalized spider diagram for subalkaline group I gabbro dykes (**a**) and subalkaline group II dolerites (**b**) and alkaline group III dolerites (**c**). N-MORB normalizing values are from Sun and McDonough (1989). The data used for comparison include OIB (Sun and McDonough 1989); Gabbro from Ladakh Himalaya (Sinha and Mishra 1994); Gabbro dykes from Kohistan island arc, Pakistan (Khan et al. 1993; Mikoshiba et al. 1999); Basaltic dyke from Kohistan island arc, Pakistan (Khan et al. 2011); Gabbros from LEG 176 (Niu et al. 2002); and Mafic dykes from Seychelles islands (Ashwal et al. 2002). The *horizontal line* in the plot shows bulk N-MORB composition

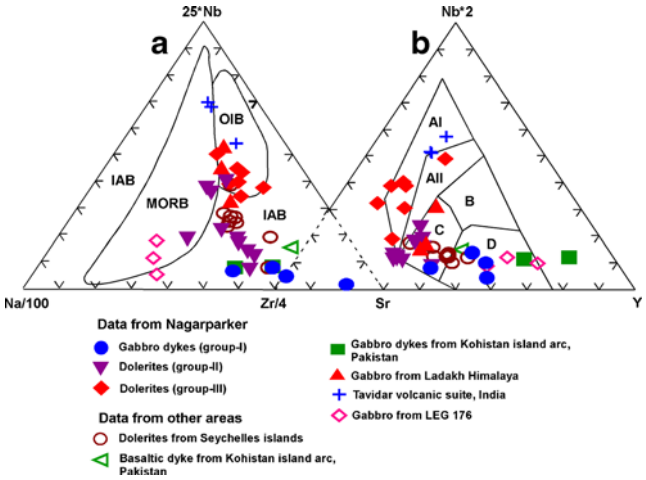

Fig. 9 **a** Discrimination diagram showing the position of subalkaline group I gabbro dykes, subalkaline group II dolerites, and alkaline group III dolerites of the Nagarparker area (after Vermeesch (2006)). The fields are defined as *IAB* island arc basalts, *OIB* ocean island basalts, and *MORB* mid ocean ridge basalts. **b** Discrimination Nb-Zr-Y diagram (Meschede 1986) for subalkaline gabbro dykes, subalkaline dolerites, and alkaline dolerites of the Nagarparker area. The fields are defined as *AI* within plate alkali basalts, *AII* within plate alkali basalts and within plate tholeiites, *B* E-type MORB, *C* within plate tholeiites and volcanic arc basalts, and *D* N-type MORB and volcanic arc basalts. Data from Tavidar volcanic suite, India, belong to Sen et al. (2012)

linked with the Seychelles islands and northwest India (e.g., Tucker et al. 2001; Torsvik et al. 2001; Ashwal et al. 2002), which formed due to the subduction of Mozambique oceanic plate underneath the continental Paleoproterozoic crust (Thomas et al. 2009). The continuation of eastern Malagasy ocean from the Betsimisaraka Suture via Bemarivo Belt to the Seychelles has also been referred in Collins and Pisarevsky (2005), Thomas et al. (2009), and Fritza et al. (2013).

On the basis of field relationship, the group I and group II dykes seem to be older than the group III dykes. The two magmatic groups possess island arc (group I and group II dykes) and OIB source (group III dykes) compositions of the Neoproterozoic and Cretaceous age, respectively, similar to Seychelles dolerites and the Tavidar volcanic suite in Eastern Rajasthan.

Conclusions

The mineralogical composition, discriminant quadratic analysis, and major and trace element variations distinguish the mafic dykes of the study area into two magmatic groups. The first group includes subalkaline gabbro dykes (group I) and dolerites (group II) showing island arc composition whereas the second magmatic group includes the OIB-type alkaline dolerites (group III). Both the magmatic groups show similarity with the mafic dykes of the Seychelles islands and the basic volcanic of the Tavidar region of Indian Rajasthan. The tentative timing of their emplacement may be Neoproterozoic and Cretaceous (?), respectively.

Acknowledgments The authors are grateful to Dr. H. Ozawa of the Naruto University of Education, Japan, for his help in the EPMA analysis and Dr. M. Q. Jan, Professor Emeritus, Pakistan, for sharing his findings related to the geology of the Nagarparker area, particularly the mafic dykes. Vice Admiral Shahid Iqbal HI (M) (Retired), Rector, Bahria University, Pakistan is thanked for facilitating this research. Dr. M. Ogasawara, Geological Survey of Japan, Okamoto K, Saitama University, Japan, are acknowledged for their contributions to improve the manuscript. Two anonymous referees are also thanked for their critical review.

References

Ahmad SM, Chaudhry MN (2007) Geochemical characterization and origin of the Karai-gabbro from the Neoproterozoic Nagarparker complex, Pakistan. Geol Bull Punjab Univ 42: 1–14

Ahmad SM, Chaudhry MN (2008) A-type granites from the Nagarparker complex, Pakistan: geochemistry and origin. Geol Bull Punjab Univ 43:69–81

Ahsan SN, Firdous R, Mastoi AS, Ghuryani S (2008) Dhedvero iron oxide-gold±copper prospect, a preliminary evaluation, Nagar Parker Taluka, Thar Parker District, Sindh, Pakistan. Geol Surv Pak Inf Release 872:1–29

Ashwal LD, Demaiffe D, Torsvik TH (2002) Petrogenesis of Neoproterozoic granitoids and related rocks from the Seychelles: the case for an Andean-type arc origin. J Petrol 43:45–83

Biswas SK (2005) A review of structure and tectonic of Kuch basin, Western India with special reference to earthquakes. Curr Sci 88: 1592–1600

Castillo PR (2006) An overview of adakite petrogenesis. Chin Sci Bull 51:257–268

Collins AS, Pisarevsky SA (2005) Amalgamating eastern Gondwana: the evolution of the Circum-Indian Orogens. Earth Sci Rev 71: 229–270

Fritza H, Abdelsalamb M, Alic KA, Bingend B, Collinse AS, Fowlerf AR, Ghebreabg W, Hauzenbergera CA, Johnsonh PR, Kuskyi TM, Macey JP, Muhongok S, Sternl RJ, Violad G (2013) Orogen styles in the East African Orogen: a review of the Neoproterozoic to Cambrian tectonic evolution. J Asian Earth Sci 86:65–106

Goutham MR, Subbarao KV, Prasad CVRK, Walsh JN, Reddy VD (2010) Proterozoic mafic dykes from the southern margin of Cuddapah Basin, India: part I—geochemistry and petrogenesis. In: Srivastava RK (ed) Dyke swarms: keys for geodynamic interpretation, 437–455. doi: 10.1007/978-3-642-12496-9_12496-9_4

Jan MQ, Laghari A, Khan MA (1997) Petrography of Nagar Parkar igneous complex, Tharparkar, southeast Sindh. Geol Bull Univ Peshawar 30:227–249

Jöns N, Schenk V, Appel P, Razakamanana T (2006) Two-stage metamorphic evolution of the Bemarivo Belt of northern Madagascar: constraints from reaction textures and in situ monazite dating. J Metamorph Geol 24:329–347

Kazmi AH, Khan RA (1973) The report on the geology, minerals and water resources of Nagar Parkar, Pakistan. Geol Surv Pak Inf Release 64:1–32

Khan MA, Jan MQ, Weaver BL (1993) Evolution of the lower crust in Kohistan, N. Pakistan: temporal arc magmatism through early, mature and intra-arc rifting. Geol Soc Lond Spec Publ 74:123–138

Khan T, Murata M, Zafar M, Rehman H (2011) Petrogenetic comparison of the mafic dykes in the Kohistan Paleo-island arc-back-arc system, Himalaya of North Pakistan. In: Srivastava RK (ed) Dyke swarms: keys for geodynamic interpretation, 437–455. doi: 10.1007/978-3-642-12496-9_24

Khan T, Murata M, Rehman H, Zafar M, Ozawaw H (2012) Nagarparker granites showing Rodinia remnants in the southeastern part of Pakistan. J Asian Earth Sci 59:39–51

Laghari A, Jan MQ, Khan MA, Agheem MH, Sahito AG, Anjum S (2013) Petrography and major element chemistry of mafic dykes in the Nagar Parkar Igneous Complex, Tharparkar, Sindh. J Himal Earth Sci 46:1–11

Maruyama S (1976) Chemical natures of the Sawadani greenstone complex in Chichibu belt, eastern Shikoku. J Geol Soc Jpn 82:183–197

Maurice C, David J, O'neil J, Francis D (2009) Age and tectonic implications of Paleoproterozoic mafic dyke swarms for the origin of 2.2 Ga enriched lithosphere beneath the Ungava Peninsula, Canada. Precambrian Res 174:163–180

Meschede M (1986) A method of discriminating between different types of mid-ocean ridge basalts and continental tholeiites with Nb-Zr-Y diagram. Chem Geol 56:207–218

Mikoshiba MU, Yutaka T, Yuhei T, Kausar AB, Khan T, Kubo K, Shirahase T (1999) Rb-Sr isotope study of the Chilas Igneous Complex, Kohistan, northern Pakistan. In: Macfarlane A, Sorkhabi RB, Quade J (eds) Himalaya and Tibet: mountain roots to mountain tops: Boulder Colorado, 328, Geol Soc Am Spec Pap., pp 47–57

Muhammad A, Alizai AH (2007) Preliminary economic evaluation of granite deposits of Nagarparker, district Tharparker, Sindh, Pakistan. Geol Surv Pak, Inf Release 861:1–12

Murata M (1993) Major and trace component analysis of Korean Institute of Energy and Resources igneous rock reference samples using X-ray fluorescence spectrometer. Res Bull Nat Sci Naruto Univ Educ Jpn 8:37–39

Muslim M, Akhtar T, Khan ZM, Khan T (1997) Geology of Nagar Parkar area, Thar Parkar district, Sindh, Pakistan. Geol Surv Pak Inf Release 605:1–21

Niu Y, Gilmore T, Mackie S, Greig A, Bach W (2002) Mineral chemistry, whole rock compositions, and petrogenesis of Leg 176 gabbros: data and discussion. In: Natland JH, Dick HJB, Miller DJ, Von Herzen RP (eds) Proceedings of the Ocean Drilling Program, Sci Result 176: 1–60

Owen-Smith TM, Ashwal LD, Torvik TH, Ganerod M, Nebel O, Web SJ, Werner SC (2013) Seychelles alkaline suite records the culmination of Deccan Traps continental flood volcanism. Lithos. doi:10.1016/j.lithos.2013.09.011

Pathan MT, Rais A (1975) Preliminary report of the investigation of Nagarparkar igneous complex. Sindh Univ J Sci 1:93–97

Pearce JA (1982) Trace element characteristics of lavas from destructive plate boundaries. In: Thorpe RS (ed) Andesites. Wiley, Chichester, pp 525–548

Raza HA, Ahmed R, Ali SM, Sheikh AM, Shafique NA (1989) Exploration performance in sedimentary zones of Pakistan. Pakistan J Hydrocarb Res 1:1–7

Sen A, Pande K, Hegner E, Sharma KK, Dayal AM, Sheth HC, Mistry H (2012) Deccan volcanism in Rajasthan: ^{40}Ar-^{39}Ar geochronology and geochemistry of the Tavidar volcanic suite. J Asian Earth Sci 59: 127–140

Sinha KA, Mishra M (1994) The existence of oceanic islands in Neotethys: evidence from Ladakh Himalaya, India. Curr Sci 67(9 and 10):721–727

Sun SS, Mcdonough WF (1989) Chemical and Isotopic Systematics of ocean basalts: implication for mantle composition and processes. In: Saunders AD, Norry MJ (eds) Magnetism in the Ocean Basins. Geol Soc Lond Spec Publ 42:313–345

Takahashi Y, Mikoshiba MU, Takahashi Y, Kausar AB, Khan T, Kubo K (2007) Geochemical modeling of the Chilas Complexin the Kohistan terrane, northern Pakistan. J Asian Earth Sci 29:336–349

Thomas RJ, Dewaele B, Schofield DL, Goodenough KM, Horstwood M, Tucker R, Bauer W, Annells R, Howard K, Walsh G, Rabarimanana M, Rafahatelo JM, Ralison AV, Randriamananjara T (2009) Geological evolution of the Neoproterozoic Bemarivo Belt, northern Madagascar. Precambrian Res 172:279–300

Torsvik TH, Ashwal LD, Tucker RD, Eide EA (2001) Neoproterozoic geochronology and paleogeography of the Seychelles microcontinent: the India link. Precambrian Res 110:47–59

Tucker RD, Ashwal LD, Torsvik TH (2001) U-Pb geochronology of Seychelles granitoids: a Neoproterozoic continental arc fragment. Earth Planet Sci Lett 187:27–38

Vermeesch P (2006) Tectonic discrimination diagrams revisited. Geochem Geophys Geosyst Am Geophys Union Geochem Soc 7:1–55

Wilson M (1989) Igneous petrogenesis. Unwin Hyman, London

Winchester JA, Floyd PA (1977) Geochemical discrimination of different magma series and their differentiation products using immobile elements. Chem Geol 20:325–343

Yoder HS, Tilley CE (1962) Origin of basalt magmas; an experimental study of natural and synthetic rock systems. J Petrol 3(3):342–529